J. Fluid Mech. (1965), *vol.* 22, *part* 1, *pp.* 81–94
Printed in Great Britain

Resolution and structure of the wall pressure field beneath a turbulent boundary layer

By W. W. WILLMARTH AND F. W. ROOS
Department of Aeronautical and Astronautical Engineering,
The University of Michigan

(Received 2 July 1964)

The power spectrum of the wall pressure that would be measured by a transducer of vanishingly small size and the corrections to the power spectra measured by finite-size transducers are determined from the spectra measured by four transducers of different diameters. The root-mean-square wall pressure measured by a transducer of vanishingly small size is $\sqrt{\overline{p^2}}/\tau_w = 2{\cdot}66$, approximately 13 % higher than the root-mean-square pressure measured by the transducer used in the earlier investigations of Willmarth & Wooldridge (1962). Corrections to the power spectrum measured by a finite-size transducer are computed using the theory of Uberoi & Kovasznay (1952, 1953). The computations require information about the correlation of the wall pressure for very small spatial separation of the transducers. Unfortunately, these measurements have never been made. Corcos's (1964) similarity of the cross-spectral density is assumed to represent the missing information, but the computed corrections fail at high frequencies because the similarity expression is not valid when the spatial separation is small. The range of validity of the similarity is determined, and the average radial derivative of the cross-spectral density is inferred from the measured power spectra.

1. Introduction

Measurements of the statistical properties of a random field made with transducers of finite size will be affected by the shape and size of the transducer. It is the purpose of this paper to investigate the effect of a finite-size circular transducer on measurements of the wall pressure beneath a turbulent boundary layer. The investigation depends upon the fact that a complete and accurate set of wall-pressure measurements can be corrected for the effect of the transducer if the transducer responds linearly to the pressure.

In the body of the paper the theory (Uberoi & Kovasznay 1952) for correcting the measurements is outlined. Computations of the corrections to the pressure are attempted using Corcos's (1964) similarity model for the measurements of Willmarth & Wooldridge (1962). The computations are inaccurate at high frequencies and cannot be improved because the set of measured data upon which everything depends is not complete (the pressure correlation at small spatial separations, $|\zeta| < 0{\cdot}7\delta^*$, of the transducers is not known).

The power spectra measured with transducers of four different diameters (Willmarth & Wooldridge 1963) are used to determine the corrections to the measured spectra. Analysis of the experimentally measured corrections of the power spectra shows that Corcos's (1964) similarity model for the cross-spectral density is not valid for spatial separations less than $0{\cdot}7\delta^*$. The average radial derivative of the cross-spectral density is determined. The paper ends with some general remarks about the effect of a finite-size transducer on the measurement of wall pressure.

2. Relations between measured and true wall pressure

The mapping of a stationary stochastic function of several variables by an instrument with a linear response has been treated by Uberoi & Kovasznay (1952, 1953) and by Liepmann (1952). The result of their work is the conclusion that, if the properties of the instrument and the mapped stochastic function are completely known, the properties of the original stochastic function can be recovered.

We present these relations in a notation appropriate to the problem of the resolution of a pressure field by a flat transducer of finite size mounted flush with a wall. The mapped stochastic property that has been measured is the pressure correlation

$$R_{pm}(\boldsymbol{\zeta},\tau) = \langle p_m(\mathbf{x},t)\, p_m(\mathbf{x}+\boldsymbol{\zeta},t+\tau)\rangle, \tag{1}$$

where the brackets indicate an average. The vectors $\boldsymbol{\zeta}(\xi,\eta)$ and $\mathbf{x}(x,y)$ lie in the plane of the wall and the subscript m denotes a measured quantity. The pressure has zero mean and is homogeneous in the plane of the wall. The measured pressure p_m is related to the true pressure p by

$$p_m(\mathbf{x},t) = \int_\infty p(\mathbf{s},t)\, K(\mathbf{s}-\mathbf{x})\, dA(\mathbf{s}), \tag{2}$$

where $K(\mathbf{s}-\mathbf{x})$ is the response kernel characterizing the spatial response of the pressure transducer. (The transducer is assumed to respond instantly to the applied pressure, and K depends only on $\mathbf{s}-\mathbf{x}$.) For a statistically homogeneous pressure field, the measured pressure correlation may then be expressed as

$$R_{pm}(\boldsymbol{\zeta},\tau) = \int_\infty\int_\infty R_p(\boldsymbol{\zeta}+\boldsymbol{\epsilon},\tau)\, K(\mathbf{s})\, K(\mathbf{s}+\boldsymbol{\epsilon})\, dA(\mathbf{s})\, dA(\boldsymbol{\epsilon}). \tag{3}$$

The essence of the problem we shall consider is the solution of this integral equation (3). The original pressure correlation $R_p(\boldsymbol{\zeta},\tau)$ is to be determined from a knowledge of $K(\mathbf{s})$ and $R_{pm}(\boldsymbol{\zeta},\tau)$. We will not actually compute R_p but will be concerned with computing the temporal Fourier transform of $R_p(0,\tau)$ (the power spectrum of the pressure).

We define the spectrum of the pressure in space and time

$$E(\mathbf{k},\omega) = \frac{1}{8\pi^3}\int_\infty\int_\infty R_p(\boldsymbol{\zeta},\tau)\exp\left[-i(\omega t+\mathbf{k}.\boldsymbol{\zeta})\right] d\tau\, dA(\boldsymbol{\zeta}), \tag{4}$$

where ω is the circular frequency and $\mathbf{k}(k_1,k_2)$ is the wave-number vector in the plane of the wall. The corresponding inverse relation is

$$R_p(\boldsymbol{\zeta},\tau) = \int_\infty\int_\infty E(\mathbf{k},\omega)\exp\left[i(\omega\tau+\mathbf{k}.\boldsymbol{\zeta})\right] d\omega\, dA(\mathbf{k}). \tag{5}$$

We will also need the cross-spectral density

$$\Gamma(\boldsymbol{\zeta}, \omega) = \frac{1}{2\pi}\int_{\infty} R_p(\boldsymbol{\zeta}, \tau) \exp(-i\omega\tau)\, d\tau, \tag{6}$$

and the power spectrum

$$\Gamma(0, \omega) = \phi(\omega). \tag{7}$$

The corresponding measured quantities $E_m(\mathbf{k}, \omega)$, $\Gamma_m(\boldsymbol{\zeta}, \omega)$, and $\phi_m(\omega)$ are defined in the same way (with the measured correlation $R_{pm}(\boldsymbol{\zeta}, \tau)$ substituted for $R_p(\boldsymbol{\zeta}, \tau)$).

In order to solve for the original power spectrum of the pressure, we must invert equation (3). We define the 'correlation' of $K(\mathbf{s})$,

$$\theta(\boldsymbol{\epsilon}) = \int_{\infty} K(\mathbf{s})\, K(\mathbf{s}+\boldsymbol{\epsilon})\, dA(\mathbf{s}), \tag{8}$$

and insert it in equation (3)

$$R_{pm}(\boldsymbol{\zeta}, \tau) = \int_{\infty} R_p(\boldsymbol{\zeta}+\boldsymbol{\epsilon}, \tau)\, \theta(\boldsymbol{\epsilon})\, dA(\boldsymbol{\epsilon}). \tag{9}$$

We recognize that the Fourier transform of a function R_{pm} which is the convolution of two functions is the product of their respective transforms. Equation (9) becomes

$$E'_m(\mathbf{k}, \tau) = 4\pi^2 E'(\mathbf{k}, \tau)\, \psi(\mathbf{k}), \tag{10}$$

where

$$E'(\mathbf{k}, \tau) = \frac{1}{4\pi^2}\int_{\infty} R_p(\boldsymbol{\zeta}, \tau) \exp(-i\mathbf{k}.\boldsymbol{\zeta})\, dA(\boldsymbol{\zeta}), \tag{11}$$

and

$$\psi(\mathbf{k}) = \frac{1}{4\pi^2}\int_{\infty} \theta(\boldsymbol{\epsilon}) \exp(-i\mathbf{k}.\boldsymbol{\epsilon})\, dA(\boldsymbol{\epsilon}). \tag{12}$$

We determine $E'(\mathbf{k}, \tau)$ from equation (10) and use the inverse of equation (11) to determine

$$R_p(\boldsymbol{\zeta}, \tau) = \frac{1}{4\pi^2}\int_{\infty} E'_m(\mathbf{k}, \tau)\, [\psi(\mathbf{k})]^{-1} \exp(i\mathbf{k}.\boldsymbol{\zeta})\, dA(\mathbf{k}). \tag{13}$$

We shall be interested in the cross-spectral density obtained from the temporal Fourier transform of equation (13)

$$\Gamma(\boldsymbol{\zeta}, \omega) = \frac{1}{4\pi^2}\int_{\infty} E_m(\mathbf{k}, \omega)\, [\psi(\mathbf{k})]^{-1} \exp(i\mathbf{k}.\boldsymbol{\zeta})\, dA(\mathbf{k}), \tag{14}$$

and the power spectrum

$$\Gamma(0, \omega) = \phi(\omega) = \frac{1}{4\pi^2}\int_{\infty} E_m(\mathbf{k}, \omega)\, [\psi(\mathbf{k})]^{-1} dA(\mathbf{k}). \tag{15}$$

$\psi(\mathbf{k})$ is the spatial 'spectrum' of the transducer and is easily computed from equation (8), where $\theta(\boldsymbol{\epsilon})$ is expressed as the convolution of $K(\mathbf{s})$. The Fourier transform of $\theta(\boldsymbol{\epsilon})$ is

$$\psi(\mathbf{k}) = \frac{1}{4\pi^2}\left[\int_{\infty} K(\mathbf{s}) \exp(-i\mathbf{k}.\mathbf{s})\, dA(\mathbf{s})\right]^2. \tag{16}$$

3. Computation of the original power spectrum from the measured pressure field

Equation (15) of the previous section gives the relation with which the original power spectrum of the pressure may be computed from quantities measured by the finite-size transducer. Measurements of the boundary-layer wall-pressure field have been reported by Willmarth & Wooldridge (1962) and more recently by Bull (1963). Corcos has used the measurements of Willmarth & Wooldridge in his work and proposed (Corcos 1962, 1963, 1964) the use of the similarity variable $\omega\zeta/U_c$ to simplify the expressions for the measured cross-spectral density. He assumes

$$\Gamma_m(\boldsymbol{\zeta}, \omega) = \phi_m(\omega)\, A(\omega\xi/U_c)\, B(\omega\eta/U_c) \exp(-i\omega\xi/U_c), \tag{17}$$

where $A(\omega\xi/U_c)$, $B(\omega\eta/U_c)$, and $U_c(\omega\delta^*/U_c)$ are reproduced from Corcos (1963) in figures 1–3. Corcos (1962 or 1964) also shows by numerical integration that

$$R_{pm}(\boldsymbol{\zeta}, \tau) = \int_\infty \phi_m(\omega)\, A(\omega\xi/U_c)\, B(\omega\eta/U_c) \exp[i(\omega\tau - \omega\xi/U_c)]\, d\omega \tag{18}$$

gives a good representation of the measured space-time correlation for the special cases $R_{pm}(\xi, 0, \tau)$ and $R_{pm}(0, \eta, 0)$.

In order to evaluate equation (15), we will use equation (17), and we need $\psi(\mathbf{k})$ for the particular transducer used in the measurements. The transducer was circular with a radius R equal to $0{\cdot}166\delta^*$ (see Willmarth & Wooldridge 1962). Therefore, if we assume that the response of the transducer is instantaneous and spatially uniform (see equation (2)),

$$\left.\begin{aligned} K(\mathbf{s}) &= 1/\pi R^2, \quad |\mathbf{s}| < R, \\ &= 0, \qquad\quad |\mathbf{s}| > R. \end{aligned}\right\} \tag{19}$$

From equation (16) we determine

$$\psi(\mathbf{k}) = (1/\pi^2)[J_1(kR)/kR]^2;\ k^2 = k_1^2 + k_2^2, \tag{20}$$

and from equation (17) we determine

$$E_m(\mathbf{k}, \omega) = \phi_m(\omega) \frac{1}{4\pi^2} \int_\infty A(\omega\xi/U_c)\, B(\omega\eta/U_c) \exp[-i(\omega\xi/U_c + \mathbf{k}.\boldsymbol{\zeta})]\, dA(\boldsymbol{\zeta}). \tag{21}$$

In the dimensionless form that we used for our computations, equation (15) can be written

$$\phi(\omega)/\phi_m(\omega) = \left(\frac{U_c}{2\pi\omega\delta^*}\right)^2 \int_{-\infty}^{\infty}\int_{-\infty}^{\infty} F_m\left(\frac{k_1^* U_c}{\omega\delta^*}, \frac{k_2^* U_c}{\omega\delta^*}\right)\left[\frac{k^*R^*}{2J_1(k^*R^*)}\right]^2 dk_1^* dk_2^*, \tag{22}$$

where $k^{*2} = k_1^{*2} + k_2^{*2}$, $k_{1,2}^* = \delta^* k_{1,2}$, $R^* = R/\delta^*$ and

$$F_m = \int_{-\infty}^{\infty}\int_{-\infty}^{\infty} A(\gamma)\, B(\beta) \exp\left[-i\left(\frac{k_1^* U_c}{\omega\delta^*} + 1\right)\gamma - i\frac{k_2^* U_c}{\omega\delta^*}\beta\right] d\gamma\, d\beta. \tag{23}$$

By a change of variables it is easy to show that ϕ/ϕ_m is a function of $\omega R/U_c$ only.

In our computations we were not able to evaluate the integral of equation (22) exactly because the zeros of $J_1(k^*R^*)$ cause it to diverge. F_m of equation (23) does not have any zeros; however, it should have zeros at the same points as

the zeros of $J_1(k^*R^*)$ because equation (10) shows that, when $\psi(\mathbf{k})$ is zero, the measured spatial spectrum $E'_m(\mathbf{k},\tau)$ should also be zero.† (If $E'(\mathbf{k},\tau)$ is finite, as it must be since R_p is not periodic and since $R_p = 0$ when $\boldsymbol{\zeta} \to \infty$, the ratio E'_m/ψ must also be finite.) The source of the difficulty is the measurement of $R_{pm}(\boldsymbol{\zeta},\tau)$. All the measurements of $R_{pm}(\boldsymbol{\zeta},\tau)$ (Willmarth & Wooldridge 1962) were made with $|\boldsymbol{\zeta}| > 0{\cdot}66\delta^*$ or $|\boldsymbol{\zeta}| > 3{\cdot}96R$. On the other hand, the transducer 'correlation', equation (8), whose spatial Fourier transform $\psi(\mathbf{k})$ produces the zeros of the measured spatial spectrum $E_m(\mathbf{k},\omega)$, is non-zero only when the spatial separation of the transducers is less than $2R$, $|\boldsymbol{\epsilon}| < 2R$. It is apparent that $\Gamma_m(\boldsymbol{\zeta},\omega)$, given in equation (17), does not contain enough experimental information about $R_{pm}(\boldsymbol{\zeta},\tau)$ to correct properly the measured power spectrum $\phi_m(\omega)$.

Putting aside these remarks for the moment, we know from Corcos (1964), for instance, that his expression for the measured cross-spectral density, equation (17), gives an acceptable representation of $R_{pm}(\xi,0,\tau)$ for $|\boldsymbol{\zeta}| > 4R$. We expect that at low frequencies the major contribution to $E_m(\mathbf{k},\omega)$ will occur at small wave numbers because the wall pressure fluctuations at low frequencies are produced by an essentially frozen large-scale eddy pattern carried past the transducer at the speed U_c. The high-wave number contribution of $E_m(\mathbf{k},\omega)$ to the low-frequency power spectrum will be negligible, and the incorrect divergent portions of the integral of equation (22), giving the corrected contributions to $\phi(\omega)$ from high wave numbers, can safely be ignored by limiting the range of integration in equation (22).

We have computed the quantity F_m of equation (23) by fitting a sum of exponential functions to Corcos's A and B. The expressions used were

$$A(\gamma) = \exp(-0{\cdot}1145|\gamma|) + 0{\cdot}1145|\gamma| \exp(-2{\cdot}5|\gamma|), \tag{24}$$

$$B(\beta) = 0{\cdot}155\exp(-0{\cdot}092|\beta|) + 0{\cdot}70\exp(-0{\cdot}789|\beta|) + 0{\cdot}145\exp(-2{\cdot}916|\beta|) + 0{\cdot}99|\beta|\exp(-4{\cdot}0|\beta|). \tag{25}$$

The fit obtained is shown in figures 1 and 2. The last terms on the right-hand side of equations (24) and (25) were chosen to make $A'(0)$ and $B'(0)$ zero. In figures 1 and 2, showing $A(\gamma)$ and $B(\beta)$, the slope at the origin is negative. Our addition of the extra term is conservative and reduces the magnitude of the spatial spectrum $E_m(\mathbf{k},\omega)$ at high wave numbers, but not significantly. We investigated the effect of omitting these two terms in the computation but found no significant change in the results or conclusions.

We have computed the integral for $\phi(\omega)/\phi_m(\omega)$ using equation (22) at four different frequencies, with $R^* = 0$, out to wave numbers $k^* \leqslant 16$ and $k^* \leqslant 18$ with the result shown in table 1.‡ The results show that at low frequencies the

† In actual experiment, $E'_m(\mathbf{k},\tau)$ may not be exactly zero because unavoidable noise will always be present in the measuring apparatus or experimental environment. The consideration of noise does not concern us here because the experimental information upon which $E'_m(\mathbf{k},\tau)$ is based is so limited (see below) that E'_m does not show any tendency to oscillate or have zeros.

‡ The integration of equation (22) was performed by weighing contours of constant F_m or $F_m[\psi(k)]^{-1}$ cut from paper of uniform thickness. The errors in this process are responsible for $\phi(\omega)/\phi_m(\omega) > 1$ at $R^* = 0$, $\omega\delta^*/U_\infty = 0{\cdot}5$.

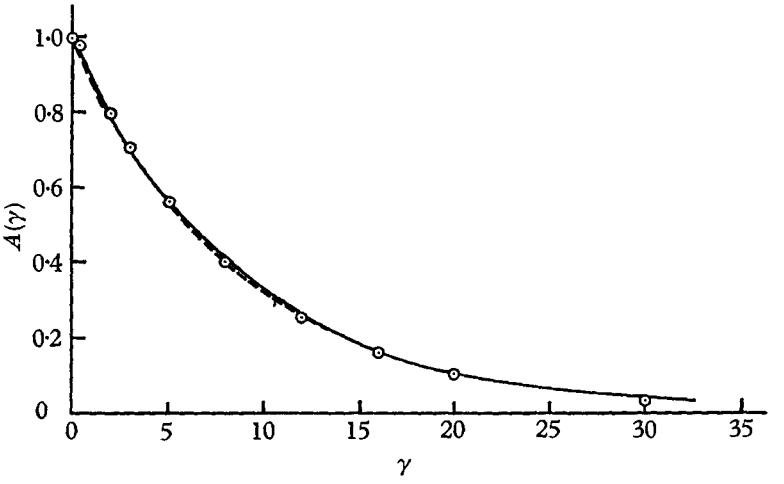

FIGURE 1. The function $A(\gamma)$, $\gamma = \omega\xi/U_c$. ———, $A(\gamma)$ determined by Corcos (1963); – – – –, exp $(-0{\cdot}1145\gamma)$; ⊙, equation (24).

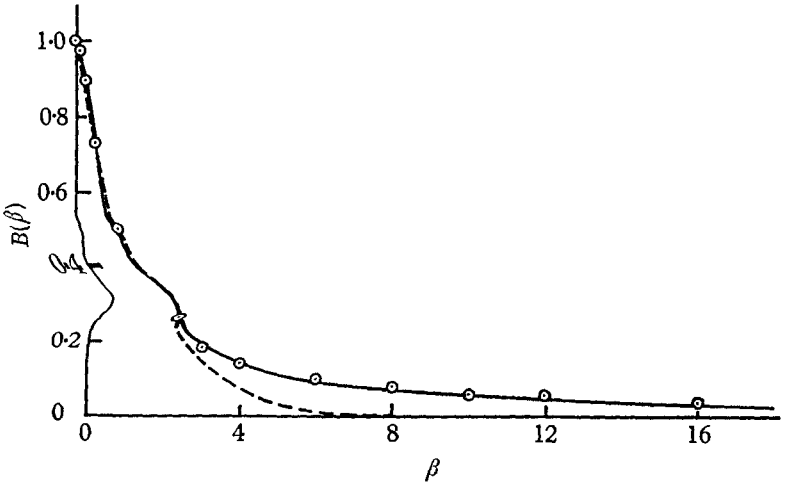

FIGURE 2. The function $B(\beta)$, $\beta = \omega\eta/U_c$. ———, $B(\beta)$ determined by Corcos (1963); – – – –, exp $(-0{\cdot}7\beta)$; ⊙, equation (25).

		$k^* \leqslant 16$		$k^* \leqslant 18$	
		$R^* = 0$	$R^* = 0{\cdot}166$	$R^* = 0$	$R^* = 0{\cdot}166$
$\omega\delta^*/U_\infty$	$\omega R/U_c$	ϕ/ϕ_m	ϕ_m/ϕ	ϕ/ϕ_m	ϕ_m/ϕ
0·5	0·109	1·023	0·957	1·024	0·952
2·0	0·468	0·970	0·758	0·980	0·700
4·0	1·006	0·824	0·627	0·870	0·488
6·3	1·660	0·626	0·535	0·694	0·389

TABLE 1. Results of computations of the ratio ϕ/ϕ_m using equation (22).

ratio $[\phi(\omega)/\phi_m(\omega)]_{R^*=0}$ is nearly one, but, as the frequency increases, more and more contributions of the spatial spectrum $E_m(\mathbf{k}, \omega)$ at high wave numbers are missing. We then computed the correction to $\phi_m(\omega)$ for $R^* = 0{\cdot}166$ and $k^* \leqslant 16$

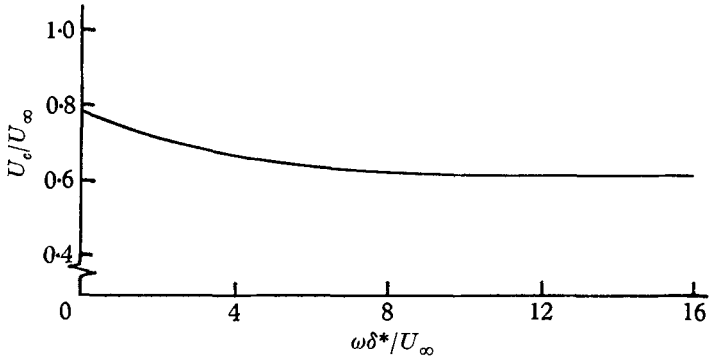

FIGURE 3. The dependence of convection velocity on frequency (Corcos 1963).

and $k^* \leqslant 18$ with the results also shown in table 1. We may place considerable confidence in the correction for $\omega\delta^*/U_\infty = 0{\cdot}5$ and possibly $2{\cdot}0$, because a correction has been applied to most of the measured spatial spectrum E_m which is included in the limited range of integration. Our confidence becomes uncertainty as $\omega\delta^*/U_\infty$ increases, and less of the measured spatial spectrum is included in the limited range of integration.

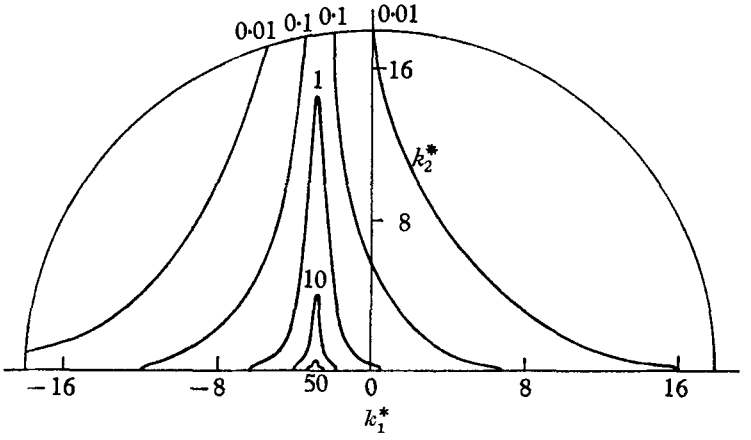

FIGURE 4. Representative contours of constant values of the integrand of equation (22) with $R^* = 0$.

An example of the character of the integrand of equation (22) is shown in figures 4 and 5 for just one frequency $\omega\delta^*/U_\infty = 2$. We see that there are ridges of large $F_m(k_1^*, k_2^*)$ extending in the k_1^* and k_2^* directions that receive a rather large correction for $k^* = 18$ (the first zero of $\psi(\mathbf{k})$ occurs at $k^* \doteqdot 23$). The error in the model for $\Gamma_m(\zeta, \omega)$ has a very serious effect for $\omega\delta^*/U_\infty \geqslant 4$.

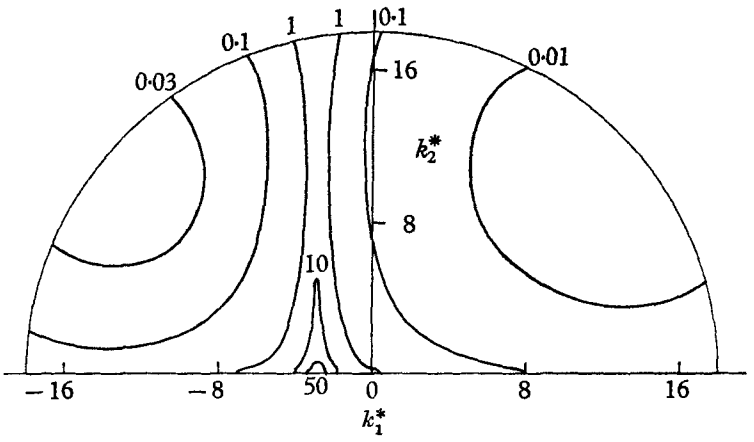

FIGURE 5. Representative contours of constant values of the integrand of equation (22) with $R^* = 0{\cdot}166$.

4. Experimental measurements with different size transducers

A suggestion by Corcos and our inability to correct properly earlier measurements of the power spectrum (Willmarth 1961) led us to measure the wall pressure spectrum (see appendix of Willmarth & Wooldridge 1963) with four circular transducers of different diameters. The results of the measurements are displayed in figures 6 and 7. The experimentally measured values of the various spectra are shown in figure 6. Smooth curves through these points were drawn, and at certain frequencies cross-plots of the spectral amplitude $\phi_m(\omega)$ as a function of transducer radius R were made from the faired curves. Extrapolated values† of $\phi(\omega)$ at $R = 0$ were obtained from the cross-plots and appear (the circled crosses) on figure 6. We have computed the area $\sqrt{\overline{p^2}}/\tau_w$ under each of the five faired spectra of figure 6 and displayed the values of $\sqrt{\overline{p^2}}/\tau_w$ on figure 7. Note that the value of $\sqrt{\overline{p^2}}/\tau_w = 2{\cdot}31$ at $R^* = 0{\cdot}166$ does not agree with our earlier value $\sqrt{\overline{p^2}}/\tau_w = 2{\cdot}19$ (Willmarth & Wooldridge 1962). We have re-examined our previous work and found errors, which we understand, in the methods of measuring $\sqrt{\overline{p^2}}/\tau_w$.‡ We attribute the scatter in the spectra at low frequencies, $\omega\delta^*/U_\infty < 1$ of figure 6, to unavoidable noise and disturbances in the wind tunnel, which had lost two turbulence screens and developed leaks and rattles that were not present previously (1962). The anomalous behaviour of the spectra above $\omega\delta^*/U_\infty = 20$ is caused by electrical noise in the amplifier of the transducer with $R/\delta^* = 0{\cdot}104$, which was made from barium titanate. The other transducers were made from lead zirconate (PZT-5) which is considerably more sensitive. The spectra of the three lead-zirconate transducers all come together above $\omega\delta^*/U_\infty = 20$ because the vibration of the tunnel wall or the pressure fluctuations from the background sound level in the wind tunnel begin to dominate those

† The variation of $\phi_m(\omega)$ with R was approximately linear as $R \to 0$. The extrapolation was not difficult nor did it appear uncertain.

‡ See the corrigendum Willmarth (1965). G. M. Corcos and M. K. Bull first pointed out this error to one of us (W. W. W.).

from the local turbulence in the boundary layer. The spatial extent of the background sound pressure or vibration field will be much greater than that of the turbulent pressure field in the boundary layer at high frequencies. Therefore, all transducers are able to resolve the sound of vibration field and the spectra should coalesce.

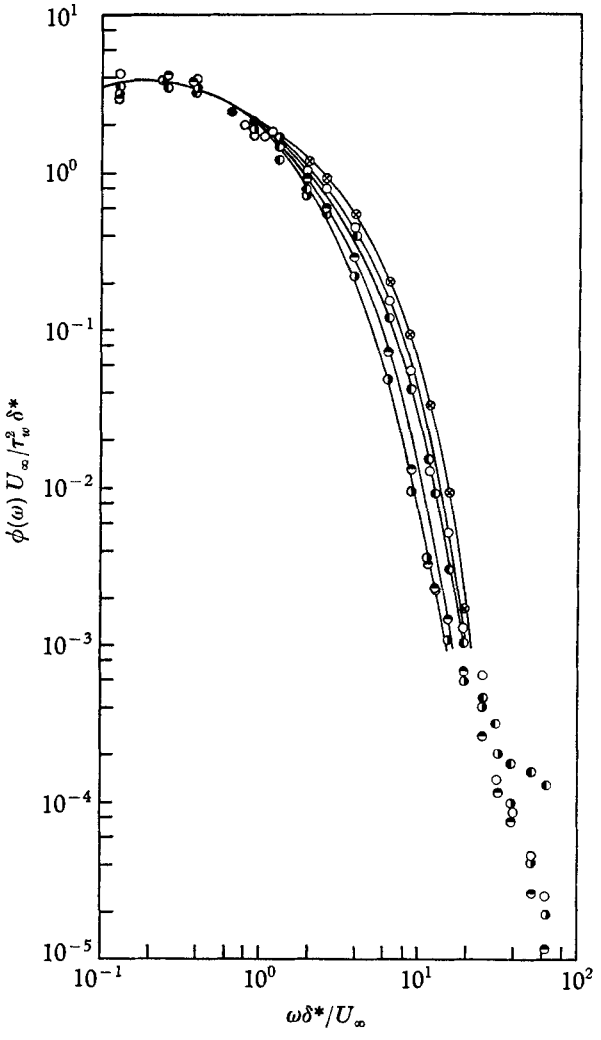

FIGURE 6. The measured and extrapolated dimensionless spectra of the wall pressure.

	R/δ^*	$\sqrt{\overline{p^2}}/\tau_w$
⊗	0·00	2·66
○	0·061	2·54
◐	0·104	2·46
◓	0·166	2·31
◑	0·221	2·20

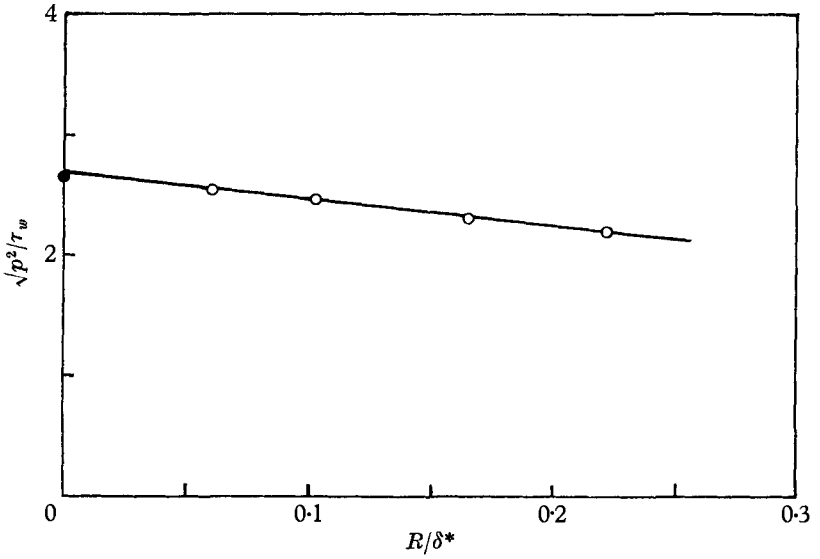

FIGURE 7. The root-mean-square wall pressure determined from the spectra of figure 6. ○, experiment; ●, from spectrum, $R/\delta^* = 0$.

5. Comparison of the experimental and computed corrections

In figure 8 we have collected the results from the computed corrections (§3, table 1) and the measured attenuation† (§4) of the wall-pressure spectra. The computed corrections for $R^* = 0{\cdot}166$ are uncertain at high frequencies, as

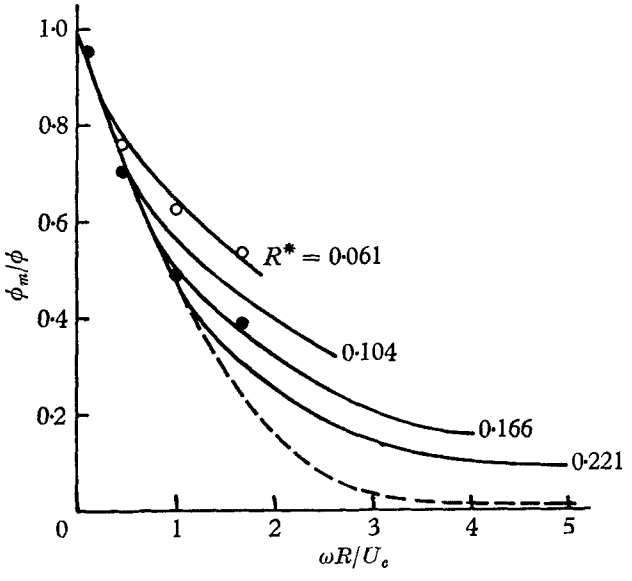

FIGURE 8. The ratio of the measured to actual power spectrum for various size transducers as a function of $\omega R/U_c$. ———, Experiment; – – – –, Corcos (1963); ○, equation (22), $R^* = 0{\cdot}166$, $k^* \leqslant 16$; ●, equation (22), $R^* = 0{\cdot}166$, $k^* \leqslant 18$.

† Data were taken from the faired curves of figure 6.

discussed in §3. The agreement between the computations with $k^* \leqslant 18$ and the experiments for $R^* = 0{\cdot}166$ at high frequencies is only a coincidence.

The experiments show the true attenuation of the wall-pressure spectra for various size transducers at the Reynolds number of the experiments, $R_\theta = 38{,}000$. The attenuation of the spectra ϕ_m/ϕ appears to be a function of $\omega R/U_c$ alone for small values of $\omega R/U_c$, but not for large values. In §3, below equation (22), we noted that ϕ_m/ϕ should be a function of $\omega R/U_c$ alone. Therefore, the assumption of a similarity expression, see equation (17), for the measured cross-spectral density that was used in equation (22) cannot be correct for all values of $\boldsymbol{\zeta}$ and ω. It is approximately correct to use the similarity for corrections to the spectra at low frequencies but not at high frequencies. More exact limitations on the similarity are discussed in §7. We note that the measured spatial spectrum $E_m(\mathbf{k}, \omega)$ should be zero for $k = \alpha_n/R^*$ at any frequency ω (see §3)†. It is clear that this behaviour cannot be obtained from the similarity expressed in equation (17).

6. Averaged properties of the derivative of the cross-spectral density, $\partial\Gamma(\boldsymbol{\zeta}, \omega)/\partial r$, for $\boldsymbol{\zeta} = 0$

Some information about the average radial derivative of the cross-spectral density can be obtained from the measurements displayed in figure 6. We consider the temporal Fourier transform of equation (9) with $\boldsymbol{\zeta} = 0$,

$$\Gamma_m(0, \omega) = \phi_m(\omega) = \int_\infty \Gamma(\boldsymbol{\epsilon}, \omega)\, \theta(\boldsymbol{\epsilon})\, dA(\boldsymbol{\epsilon}). \tag{26}$$

For a circular transducer $\theta(\boldsymbol{\epsilon})$ (the 'correlation' of $K(\mathbf{s})$ in equation (8)) is proportional to the overlapping areas of two circles whose centres are separated by a distance ϵ

$$\left.\begin{aligned} \theta(\boldsymbol{\epsilon}) &= \frac{2}{\pi^2 R^2}\left[\cos^{-1}\frac{\epsilon}{2R} - \frac{\epsilon}{2R}\sqrt{\left\{1 - \left(\frac{\epsilon}{2R}\right)^2\right\}}\right], \quad |\boldsymbol{\epsilon}| = \epsilon \leqslant 2R, \\ &= 0 \qquad\qquad\qquad\qquad\qquad\qquad\qquad\quad \epsilon > 2R. \end{aligned}\right\} \tag{27}$$

Equation (26) becomes

$$\phi_m(\omega, R) = \frac{8}{\pi^2}\int_0^{2\pi}\int_0^1 \Gamma(2R\alpha, \theta, \omega)\, [\cos^{-1}\alpha - \alpha\sqrt{(1-\alpha^2)}]\, \alpha\, d\alpha\, d\theta, \tag{28}$$

and the derivative with respect to R at $R = 0$

$$\left[\frac{\partial\phi_m(\omega, R)}{\partial R}\right]_{R=0} = \frac{32}{\pi}\left\{\int_0^1 [\cos^{-1}\alpha - \alpha\sqrt{(1-\alpha^2)}]\, \alpha^2\, d\alpha\right\}\left\{\frac{1}{2\pi}\int_0^{2\pi}\left\langle\frac{\partial\Gamma}{\partial r}\right\rangle_{r=0} d\theta\right\}, \tag{29}$$

where $r^2 = \xi^2 + \eta^2$. Evaluating the integral and normalizing, we obtain

$$\left[\frac{\partial\phi_m(\omega)/\phi(\omega)}{\partial R}\right]_{R=0} = \frac{384}{135\pi}\left\langle\frac{\partial \ln\Gamma}{\partial r}\right\rangle_{r=0} \doteqdot 0{\cdot}906\left\langle\frac{\partial \ln\Gamma}{\partial r}\right\rangle_{r=0}. \tag{30}$$

We show $\langle\partial \ln\Gamma/\partial(\omega r/U_c)\rangle_{r=0}$, determined from experimental values of $\partial\phi_m/\partial R$ using equation (30) and figure 6, in figure 9. In figure 9 we have also shown

† α_n ($n = 1, 2, \ldots$) are the zeros of $J_1(\alpha)$.

$\langle \partial \ln \Gamma / \partial r / \delta^* \rangle_{r=0}$ in order to display this quantity as a function of a length characteristic of the boundary layer rather than the wavelength $2\pi U_c/\omega$, whose meaning and interpretation is doubtful when ζ is small (see §7).

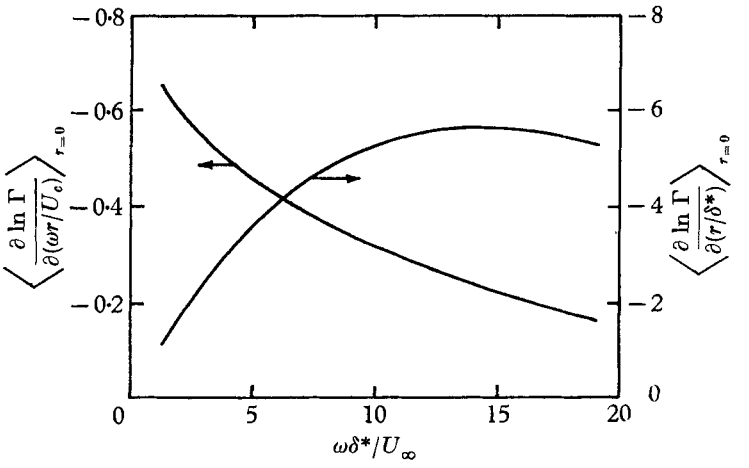

FIGURE 9. Experimentally determined average value of the derivative of the cross-spectral density at $\zeta = 0$ as a function of dimensionless frequency.

7. Range of validity of the Corcos similarity hypothesis

The ratio $\phi_m(\omega)/\phi(\omega)$ measured with different diameter transducers is not a function of $\omega R/U_c$ alone. If the measured cross-spectral density is similar, in the manner proposed by Corcos (1964) and expressed in equation (17), the attenuation of the power spectrum ϕ_m/ϕ would be a function of $\omega R/U_c$ alone (see §5).

From the measurements shown in figure 8, the lack of similarity (dependence on $\omega R/U_c$ alone) occurs at larger values of $\omega R/U_c$ when the transducer diameter increases. $2\pi U_c/\omega$ is the characteristic wavelength λ of the component of the convected pressure field that produces a pressure fluctuation of frequency $\omega/2\pi$. The value of the dimensionless parameter $\omega R/U_c$ at which the curve $\phi_m(\omega)/\phi(\omega)$ of figure 8, for a given transducer, departs from the common curve describing the attenuation of the remaining transducers indicates the frequency above which the transducer attenuation no longer obeys the similarity hypothesis. The approximate wavelength of the convected pressure pattern below which similarity is no longer obtained is then $\lambda/\delta^* \doteqdot 2\pi R^*[\omega R/U_c]^{-1}$. From figure 8 this value of λ/δ^* is 1·4 for $R^* = 0{\cdot}166$, 1·3 for $R^* = 0{\cdot}104$, and 1·5 for $R^* = 0{\cdot}061$. From an average of these values of λ/δ^*, we conclude that for spatial separations of the order $\frac{1}{2}\lambda = 0{\cdot}7\delta^*$ or less, Corcos's similarity hypothesis is not valid when (as in the above discussion) the dimensionless frequency is greater than approximately three, $\omega\delta^*/U_\infty > 3$. We do not mean to imply that there is any basic contradiction to Corcos's work (Corcos 1964), since the experimental evidence for the similarity is obtained from measurements with $|\zeta| > 0{\cdot}66\delta^*$, and Corcos (1964) discusses the fact that for small $\omega\xi/U_c$ there is no strong support for the similarity.

Another way to demonstrate the lack of similarity for small $|\zeta|$ is to note that, if the original cross-spectral density were similar in the sense of equation (17), the average normalized radial derivative $\langle \partial \ln \Gamma / \partial r \rangle_{r=0}$ can be computed. Using equation (17) and the last term on the right of equation (29), the average radial derivative becomes

$$\left\langle \frac{\partial \ln \Gamma}{\partial (\omega r/U_c)} \right\rangle_{r=0} = \frac{2}{\pi}[A'(0) + B'(0)]. \tag{31}$$

Equation (31) is a constant as a direct consequence of the similarity expressed in equation (17). From the results shown in figure 9 it is apparent that

$$\langle \partial \ln \Gamma / \partial(\omega r/U_c) \rangle_{r=0}$$

is not constant indicating that the similarity does not exist for vanishingly small ζ and frequencies above $\omega\delta^*/U_\infty = 1{\cdot}0$.

To complete this discussion of the validity of the similarity, we note that Bull (1963) and Bull *et al.* (1963) have measured the wall pressure correlation in narrow frequency bands for a wide range of frequencies and for $|\zeta| \geqslant 0{\cdot}82\delta^*$. They found (Bull 1963, figures 16 and 17, and Bull *et al.* 1963) that for low frequencies the similarity was not valid. According to the data there were departures from similarity for dimensionless frequencies $\omega\delta^*/U_\infty$ less than approximately one and spatial separations greater than δ^*.

Consider the quarter-infinite region $0 < \omega\delta^*/U_\infty < \infty$, $0 < |\zeta|/\delta^* < \infty$. From our results and the measurements by Bull (1963) and Bull *et al.* (1963) the similarity expressed by equation (17) is not valid at the origin ($\omega = \zeta = 0$) and in the regions $\omega\delta^*/U_\infty > 3$, $|\zeta|/\delta^* < 0{\cdot}7$ and $\omega\delta^*/U_\infty < 1$, $|\zeta|/\delta^* > 1$.

8. Additional remarks about the effect of finite size

It is natural to ask whether the similarity (expressed in equation (17)) of the original cross-spectral density $\Gamma(\zeta, \omega)$ would be destroyed by measuring Γ with a finite-size transducer. We suppose that Γ possesses the similarity expressed in equation (17) and that A and B are exponential functions; $\gamma, \beta > 0$. Γ_m is determined from the temporal Fourier transform of equation (9). Then, because A and B are even functions of their arguments and because $\theta(\epsilon)$ is a function of ϵ/R (being zero for $\epsilon \geqslant 2R$, see equation (27)), the original similarity of Γ is destroyed for spatial separations $|\xi| < 2R$ or $|\eta| < 2R$ but is retained if $|\xi| > 2R$ and $|\eta| > 2R$. If A and B are not represented by exponential functions the original similarity is lost for all spatial separations. It is not possible to make a general statement about the amount of destruction of the original similarity. One must consider a specific expression for $\Gamma(\zeta, \omega)$.

We can state that it will be difficult to learn much about the cross-spectral density when the separation is small, because the experimental measurements must be made with specially shaped (intersecting circular or square) transducers and then corrected for the effects of the finite size of the transducer. It would be best to make the transducer size as small as possible for this type of investigation.

9. Conclusions

(1) The attenuation of the power spectrum of the wall pressure has been experimentally measured for circular transducers of four different diameters.

(2) The root-mean-square wall pressure that would be measured by a vanishingly small transducer is $\sqrt{\overline{p^2}} = 2{\cdot}66\tau_w$ when the Reynolds number based on the momentum thickness $R_\theta = 38{,}000$.

(3) Corcos's conclusion (Corcos 1963, 1964) that transducers used in contemporary measurements were unable to resolve a large fraction of the total pressure signal is incorrect. In one set of measurements (Willmarth & Wooldridge 1962), the unresolved root-mean-square pressure was 13% of the total root-mean-square pressure signal.

(4) Existing measurements of the wall pressure correlation with finite-size transducers have not been made at small enough spatial separations between the transducers to allow accurate computation of the loss of resolution at high wave-numbers or frequencies.

(5) The average radial derivative of the normalized cross-spectral density has been determined from the measurements of the attenuation of the power spectrum and is not proportional to U_c/ω as required by the similarity proposed by Corcos (1964).

(6) The similarity proposed by Corcos (1964) is not valid for spatial separations less than approximately $0{\cdot}7\delta^*$, and dimensionless frequencies above three. From the work of Bull (1963, figures 16 and 17) and Bull *et al.* (1963) the similarity is not valid when the dimensionless frequency is less than approximately one, and the spatial separation greater than approximately δ^*.

The authors wish to thank Professor M. S. Uberoi for many valuable discussions and suggestions. This work was initiated at the University of Michigan and was supported by the Office of Naval Research under contract no. Nonr 1224(30). It was completed during a portion of the senior author's Visiting Fellowship at the Joint Institute for Laboratory Astrophysics.

REFERENCES

Bull, M. K. 1963 *University of Southampton A.A.S.U., Rep.* no. 234.

Bull, M. K., Wilby, J. F. & Blackman, D. R. 1963 *University of Southampton A.A.S.U., Rep.* no. 243.

Corcos, G. M. 1962 *University of California Inst. of Eng. Res. Rep., Series* 183, no. 2.

Corcos, G. M. 1963 *J. Acoust. Soc. Amer.* **35.**

Corcos, G. M. 1964 *J. Fluid Mech.* **18**, 353.

Liepmann, H. W. 1952 *Z. angew. Math. Phys.* **3**, 322.

Uberoi, M. S. & Kovasznay, L. S. G. 1952 *Johns Hopkins University Project Squid Tech. Rep.* no. 30.

Uberoi, M. S. & Kovasznay, L. S. G. 1953 *Quart. Appl. Math.* **10**, 375.

Willmarth, W. W. 1961 *WADC Tech. Rep.* no. 59–676 109.

Willmarth, W. W. 1965 *J. Fluid Mech.* **21**, 107.

Willmarth, W. W. & Wooldridge, C. E. 1962 *J. Fluid Mech.* **14**, 187.

Willmarth, W. W. & Wooldridge, C. E. 1963 *AGARD Rep.* no. 456.